$2\pi/3$ Me_3Sn Propeller-Like Jumps in Solid Bis(trimethyltin)–Dimesylamide–Hydroxide, $[Me_3Sn\{\mu\text{-}(MeSO_2)_2N\}Me_3Sn(\mu\text{-}OH)]_n$

Jörg Kümmerlen, Ilona Lange,† Wolfgang Milius,‡ Angelika Sebald,* and Armand Blaschette†

Bayerisches Geoinstitut, Universität Bayreuth, 95440 Bayreuth, Germany

Received March 8, 1993®

Rates and activation energies of $2\pi/3$ propeller-like jumps for the two inequivalent Me_3Sn sites in solid crystalline $[Me_3Sn\{\mu\text{-}MeSO_2)_2N\}Me_3Sn(\mu\text{-}OH)]$, **1**, as obtained from variable temperature one- and two-dimensional ^{13}C CP/MAS NMR, are discussed in comparison to the single crystal X-ray structure of **1** at 296 and 178 K and in conjunction with force field considerations (atom–atom potential energy barrier calculations). The combined results allow assignment of the two resonances in the ^{119}Sn CP/MAS spectra of **1** to the specific molecular Me_3Sn sites in **1** and give evidence as to what structural features in **1** are responsible for the two different energy barriers of the observed $2\pi/3$ Me_3Sn propeller-jump processes.

Introduction

Trimethyltin compounds Me_3SnX tend to form crystalline polymeric zigzag chains in the solid state.[1] For ligands X where oxygen provides the coordinating atom (for example X = OH^-, CO_3^{2-}, $MeCO_2^-$, etc.) this polymerization in the solid state leads to more or less distorted trigonal-bipyramidal 5-fold Me_3SnO_2 coordination with oxygen atoms occupying the axial positions. Using one- and two-dimensional variable temperature ^{13}C and ^{119}Sn CP/MAS methods, we have recently shown for a series of such polymeric trimethyltin compounds that $2\pi/3$ propeller-like jumps of the Me_3Sn unit around the O–Sn–O axis seem to be a fairly common process in the solid state.[2] Depending on the ligand X, we have observed activation energies for this Me_3Sn reorientational process in the range 38.6–72.5 kJ mol^{-1}.

The title compound $[Me_3Sn\{\mu\text{-}(MeSO_2)_2N\}Me_3Sn(\mu\text{-}OH)]_n$, **1**, belongs to this category of chain-building trimethyltin compounds, the low temperature X-ray crystal structure has been described,[3] and **1** shows different jump rates and activation energies for the $2\pi/3$ Me_3Sn reorientation of the two inequivalent Me_3Sn sites in solid **1** (38.6 and 44.8 kJ mol^{-1}, respectively[2]). NMR spectroscopy alone cannot explain why there should be different activation energies for this process at the two different Me_3Sn sites. The low temperature (178 K) X-ray single crystal structure of **1**[3] does not readily reveal why considerable Me_3Sn $2\pi/3$ jump rates at room temperature are possible at all, neither is it possible to assign the two resonances in the ^{119}Sn CP/MAS spectra of **1** to specific Me_3Sn sites. We have speculated[2] that possibly the Sn(1)–(OH)–Sn(2) bond angle in solid **1** may change as a function of temperature, i.e. increase with increasing temperature, and thus may allow relatively high Me_3Sn reorientational jump rates for **1** at room temperature.

To further investigate this structure–dynamic process relationship, the single crystal X-ray structure of **1** has been redetermined at room temperature. On the basis of the crystal structure data at low and at room temperature, force field calculations considering van der Waals interactions[4] have been carried out and have been used as a qualitative tool to rationalize the observed energy barriers in terms of structural parameters. The combined results from X-ray crystallography, high-resolution solid-state NMR, and force field considerations on **1** will be discussed in the following.

Experimental Section

All experimental details concerning ^{13}C and ^{119}Sn CP/MAS NMR of **1** are given in ref 2; the synthesis and the low temperature single crystal X-ray structure of **1** are described in ref 3.

Single Crystal X-ray Structure Determination of 1 at T = 296 K. The data collection was carried out on a Siemens P4 single crystal diffractometer using a colorless plate-shaped crystal of **1** (0.22 × 0.20 × 0.10 mm^3) contained in a glass capillary. A total of 3690 intensities were collected up to $2\theta_{max}$ = 50°; 3048 reflections were independent with R_{int} = 3.38% and significant ($F > 0.0\sigma(F)$). Cell parameters were refined on the basis of 42 reflections in the 2θ range $28° \le 2\vartheta \le 30°$. An empirical correction for absorption was carried out by ψ-scans with transmission factors of 0.68–0.87. The structure was solved using direct methods[5] and was refined anisotropically to R = 0.0392 (R_w = 0.0281). Methyl groups were treated assuming idealized geometries. The weighting scheme used was $w^{-1} = \sigma^2(F) + 0.0000F^2$. An extinction correction with $F^* = F[1 + 0.002F^2/\sin 2\theta]^{-1/4}$ yielded a refined value for x = 0.000 33(3); 164 parameters, Δ/σ_{max} = 0.001, $\Delta\rho_{max}$ = 1.71 × 10^{-6} e pm^{-3}, $\Delta\rho_{min}$ = −0.99 × 10^{-6} e pm^{-3}. The atom numbering scheme is given in Figure 1; a full listing of all structural parameters is available as supplementary material.

Atom–Atom Potential Energy Barrier Calculations. The calculations were performed using the program Moby, V.1.4,[6]

† Institut für Anorganische und Analytische Chemie, Technische Universität, Hagenring 30, 38106 Braunschweig, Germany.

‡ Laboratorium für Anorganische Chemie, Universität Bayreuth, 95440 Bayreuth, Germany.

® Abstract published in *Advance ACS Abstracts*, August 15, 1993.

(1) (a) Molloy, K. C. In *Chemistry of Tin*; Harrison, P. G., Ed.; Blackie: Glasgow and London, 1989; pp 187–220. (b) Tiekink, E. R. T. *Appl. Organomet. Chem.* **1991**, *5*, 1.

(2) Kümmerlen, J.; Sebald, A. *J. Am. Chem. Soc.* **1993**, *115*, 1134.

(3) Blaschette, A.; Wieland, E.; Jones, P. G.; Hippel, I. J. *Organomet. Chem.* **1993**, *445*, 55.

(4) Rappé, A. K.; Casewitt, C. J.; Colwell, K. S.; Goddard, W. A., III; Skiff, W. M. *J. Am. Chem. Soc.* **1992**, *114*, 10024.

(5) Sheldrick, G. M. *SHELXTL PLUS V.4.2*; Crystallographic System, Siemens Analytical X-ray Instruments Inc.: Madison, WI, 1992.

(6) Springer New Media; Springer-Verlag: Berlin, Heidelberg, New York, Tokyo, 1991.

0276-7333/93/2312-3541$04.00/0

with a 12–6 Lennard–Jones-type potential.[7] A van der Waals radius vdW_{Sn} of 2.17 Å[8] and a well depth of 0.3 kcal mol^{-1} were assumed. The choice of the vdW parameters for the tin atoms is not a crucial point since all Sn–O and Sn–C bond lengths and bond angles remain unaltered over the entire calculation procedure: any misadjustment of the vdW parameter would result in a shift of the complete potential energy profile but would affect neither the shape nor the amplitude/"height" of the energy barrier.[9,10] In order to take the fast internal reorientation of the various methyl groups into account, all methyl groups are treated as "pseudoatoms" with a vdW radius of 2 Å ("united atom description"). Such pseudoatoms are implemented in the Moby program. For our calculation purposes a rigid Me_3Sn rotor in a noncooperative crystal environment was assumed. This assumption leads to potential energy barrier heights which are the upper limit of the true potential energy barrier heights. As is obvious from the X-ray crystal data, in compound 1 the methyl groups of both Me_3Sn units interact with methyl groups from Me_3Sn units of the neighboring chain in their mutual relative orientation with the highest vdW interaction energy. Since all Me_3Sn units in 1 undergo reorientation, though with differing jump rates, the "time averaged" potential energy barrier must be lower than the calculated one. An 8-Å cutoff distance was used for the calculations, the basis of the calculations was a 25- × 25- × 25-Å cube. Only the Cartesian coordinates of atoms other than hydrogen were used as input, the positions of the hydrogen atoms of the bridging OH groups were added using symmetry considerations, and an O–H bond length of 0.96 Å was assumed. Calculations of one-dimensional potential energy profiles for both Me_3Sn units were carried out by rotating the respective Me_3Sn unit in 8-deg steps around the respective Sn–O(5) bond, while leaving the other Me_3Sn unit in its equilibrium position. A complete range of orientations around the crystallographic equilibrium position ($\theta = 0°$) of $-180° \leq \theta \leq 180°$ was covered for $Me_3Sn(1)$ and $Me_3Sn(2)$. The two-dimensional mutually orientation dependent potential energy profile of the $Me_3Sn(2)$ unit as a function of the displacement of the $Me_3Sn(1)$ orientation from its crystallographic equilibrium position was obtained in 8-deg steps for the $Me_3Sn(2)$ unit (covering $-180° \leq \theta_2 \leq 180°$), and in 16-deg steps for $Me_3Sn(1)$ (covering $-64° \leq \theta_1 \leq 160°$). The results of these calculations are illustrated in Figures 4 and 5, respectively.

Results and Discussion

On the basis of the results of the low temperature (T = 178 K) X-ray single crystal structure determination,[3] the structure of solid 1 is best described as infinite chains built from alternating $[(Me_3Sn(1))(OH)(Me_3Sn(2))]^+$ cations and α,ω-bridging dimesylamide anions $[(MeSO_2)_2N]^-$:

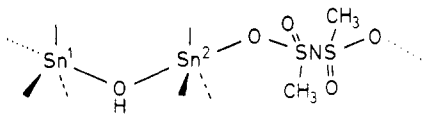

Within these chains the two independent tin atoms are located in slightly distorted trigonal-bipyramidal Me_3SnO_2 coordination. The low temperature X-ray crystal structure also shows that neighboring antiparallel chains are linked by Sn–O(5)H···N hydrogen bonds, thus forming a ladder-type structure. Considering the results obtained from the room temperature X-ray structure determination, we find that most low temperature structural features of 1 are retained at room temperature. At room temperature (296 K) again we find two independent tin atoms in slightly distorted trigonal-bipyramidal coordination. The Sn(1,2)–O(H) distances of 212.3(4) and 211.9(4) pm have to be considered as representing typical covalent bonds (the sum of covalent radii SnO is 214 pm[11]). The Sn(1)–(OH)–Sn(2) angle is 138.2(2)°, and all Sn(1,2)–C distances are close to 211 pm. C–Sn(1,2)–C angles ranging from 116.8(2) to 120.0(3)° are found. Both C_3SnO_2 trigonal bipyramids deviate slightly from an ideal geometry: O(H)–Sn(1,2)–C bond angles ranging from 95.5(2) to 97.8(2)° deviate from the ideal value of 90°; both O–Sn(1,2)–O axes are not precisely linear (174.7 and 173.5°, respectively). All these bond lengths and angles for 1 are, within standard deviations, identical at 178 and 296 K.

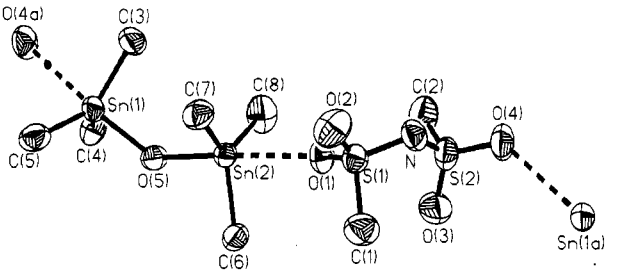

Figure 1. ORTEP plot of the section of the chain structure of 1 representing one molecular unit, as obtained from the single crystal X-ray structure determination at T = 296 K. The atom numbering scheme is shown.

Significant differences between the structures of 1 at these two temperatures are observed for the ionic contact between the $[(Me_3Sn)_2OH]^+$ cation and the $[(MeSO_2)_2N]^-$ anion: the Sn(2)–O(1) distance is 253.3(2) pm at 178 K and increases to 258.3(3) pm at 296 K, resulting in a stretching of the chain along the (110) direction. No such significant change is observed for Sn(1). Also the length of the hydrogen-bonding interaction between two neighboring chains, O(5)H···N increases from 294 pm (178 K) to 302 pm (296 K). This is reflected by the increased cell dimensions at room temperature:

T, K	178	296
a, pm	825.4(3)	841.7(2)
b, pm	856.2(3)	851.6(2)
c, pm	1341.6(5)	1375.6(3)
α, deg	81.97(3)	82.07(3)
β, deg	74.72(3)	73.89(3)
γ, deg	79.75(3)	79.67(3)

The atom numbering scheme and the asymmetric unit of 1 at T = 296 K are illustrated in Figure 1.

A summary of ^{13}C and ^{119}Sn CP/MAS results[2] on 1 yields the following information. In agreement with the X-ray diffraction results, the ^{119}Sn CP/MAS spectrum of 1 at room temperature displays two ^{119}Sn resonances with $\delta(^{119}Sn)$ = 94.8 and 68.6 ppm, respectively (see Figure 2). The high-frequency ^{119}Sn resonance shows a moderately temperature-dependent isotropic ^{119}Sn chemical shift ($\Delta\delta$ = 0.06 ppm K^{-1}) in the temperature range 200–263 K, while the low-frequency ^{119}Sn resonance shifts considerably with temperature ($\Delta\delta$ = 0.15 ppm K^{-1}). At low temperature (T = 243 K) six sharp ^{13}C resonances for the two Me_3Sn units are observed. ^{13}C 2D exchange experiments allow us to subdivide these six resonances into two groups of

(7) Destro, R.; Gavezzotti, A. In *Structure and Properties of Molecular Crystals*; Pierrot, M., Ed.; Studies in Physical and Theoretical Chemistry; Elsevier: Amsterdam, 1990; Vol. 69, pp 161–210.
(8) Harrison, P. G. In *Chemistry of Tin*; Harrison, P. G., Ed.; Blackie: Glasgow and London, 1989; p 10.
(9) Braga, D.; Grepioni, F.; Parisini, E. *Organometallics* **1991**, *10*, 3735.
(10) Braga, D. *Chem. Rev.* **1992**, *92*, 633.
(11) Omae, I. Organotin Chemistry. *J. Organomet. Chem. Libr.* **1989**, *21*, 238.

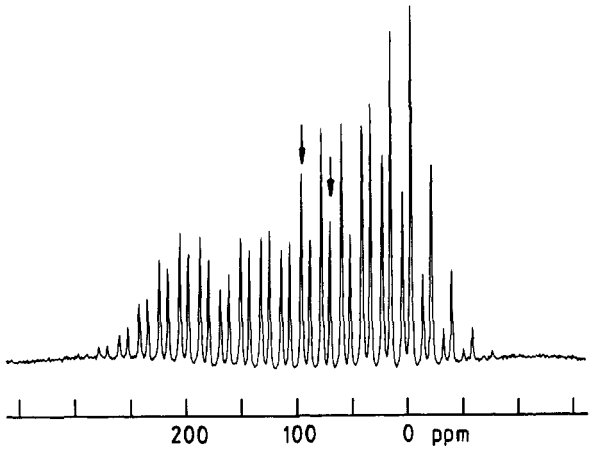

Figure 2. Room temperature 111.9-MHz ^{119}Sn CP/MAS spectrum of **1**: ν_{rot} = 2.05 kHz, 400 transients.

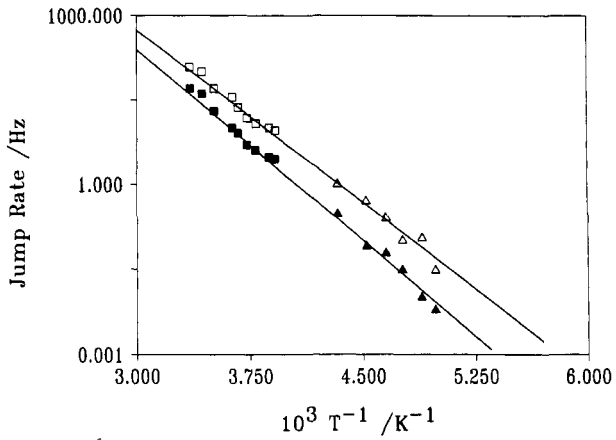

Figure 3. Arrhenius plot based on the $2\pi/3$ jump rates obtained from ^{13}C NMR[2] for $Me_3Sn(1)$ and $Me_3Sn(2)$ in **1**. Data from 2D ^{13}C exchange experiments: △ ≙ $Me_3Sn(2)$, ▲ ≙ $Me_3Sn(1)$. Data from 1D ^{13}C lineshape analysis: □ ≙ $Me_3Sn(2)$, ■ ≙ $Me_3Sn(1)$. From this set of data, activation energies of E_a = 44.8 ± 3 kJ mol^{-1} ($Me_3Sn(1)$) and 38.6 ± 3 kJ mol^{-1} ($Me_3Sn(2)$) are obtained.

three ^{13}C resonances (4.5, 2.5, 0.0 ppm and 4.1, 2.7, −1.2 ppm at T = 243, respectively). Variable temperature ^{13}C one- and two-dimensional exchange spectroscopy yields the respective $2\pi/3$ jump rates for the two independent Me_3Sn units as a function of temperature. This is shown in Figure 3. The Arrhenius plot in Figure 3 illustrates that the jump rates for $Me_3Sn(1)$ and $Me_3Sn(2)$ in **1** are significantly different over the entire accessible range, and we observe Arrhenius-type behavior for all accessible jump rates. Meaningful jump rates at temperatures below 200 K could not be obtained from ^{13}C 2D exchange experiments due to increasing signal-to-noise problems for the off-diagonal peaks and due to the onset of T_1-related losses of ^{13}C magnetization during the necessary (long) mixing times.

Combining the variable temperature X-ray and NMR evidence, we can now assign the two ^{119}Sn resonances to Sn(1) and Sn(2). Given the expressed temperature dependence of the lower-frequency ^{119}Sn resonance and the significant structural changes from 178 K to room temperature for Sn(2), the ^{119}Sn resonance at 68.6 ppm must be assigned to Sn(2). Sn(1) corresponds to the ^{119}Sn resonance at 94.8 ppm. It also seems reasonable to assign the faster $2\pi/3$ Me_3Sn reorientation process to this $Me_3Sn(2)$ unit (i.e. ^{13}C resonances at 4.5, 2.5, 0.0 ppm at T = 243 K), but this latter assignment needs further corroboration from force field calculations.

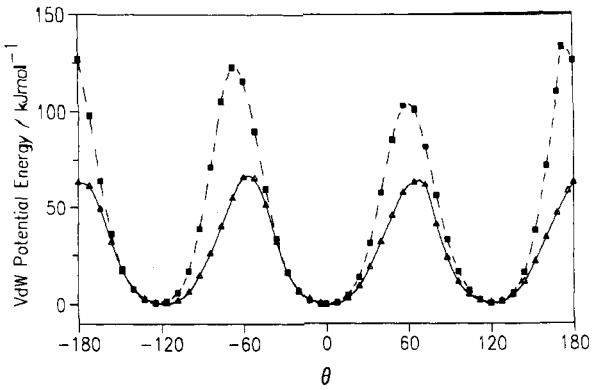

Figure 4. Relative potential energy (kJ mol^{-1}) for $Me_3Sn(1)$ (■) and $Me_3Sn(2)$ (△) in solid **1** at 296 K. θ = 0 corresponds to the crystallographic equilibrium position.

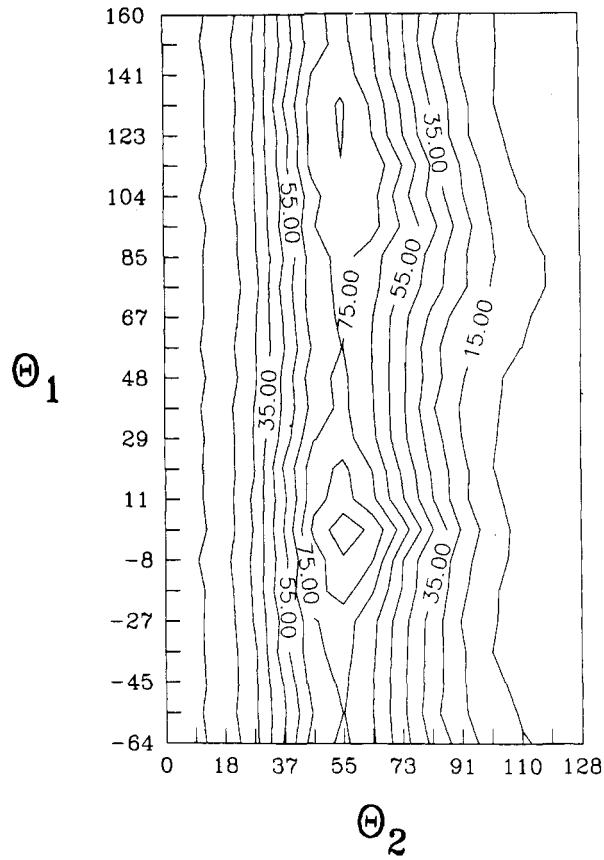

Figure 5. Contour plot in 10 kJ mol^{-1} steps of the potential energy barrier height of $Me_3Sn(2)$ as a function of the relative orientation of $Me_3Sn(1)$ in solid **1** at T = 178 K. θ = 0 corresponds to the respective crystallographic equilibrium positions. Only the regions $0° \le \theta_2 \le 128°$ and $-64° \le \theta_1 \le 160°$ is shown.

Force field calculations for **1** at room temperature yield potential energy profiles for the $2\pi/3$ jump process which show significantly different potential heights for $Me_3Sn(1)$ and $Me_3Sn(2)$ (see Figure 4). Calculations based on the low temperature X-ray crystal structure also show quite different potential heights for $Me_3Sn(1)$ and $Me_3Sn(2)$. At both temperatures the potential energy barrier height for the $Me_3Sn(2)$ moiety (E_p = 101 kJ mol^{-1} at T = 178 K, E_p = 67 kJ mol^{-1} at T = 296 K) is considerably lower than for the $Me_3Sn(1)$ unit (E_p = 185 kJ mol^{-1} at T = 178 K, E_p = 125 kJ mol^{-1} at T = 296 K). This finding fully

supports that we observe different $2\pi/3$ jump rates for $Me_3Sn(1)$ and $Me_3Sn(2)$ over the entire temperature range accessible to NMR. Furthermore, within the limits of potential energy calculations, also the tentative "jump-rate" ^{13}C assignment of the six methyl ^{13}C resonances as discussed above is supported.

Figure 5 shows a two-dimensional plot of the potential energy profile of the faster reorienting $Me_3Sn(2)$ unit versus the orientation displacement of the slower reorienting $Me_3Sn(1)$ unit. This calculation shows that T = 178 K the potential energy height of the $Me_3Sn(2)$ unit is modulated by the orientation of the $Me_3Sn(1)$ unit by approximately 30%. The situation is quite different for the room temperature structure of 1 where the influence of the $Me_3Sn(1)$ orientation on the potential energy height of $Me_3Sn(2)$ amounts to only approximately 10%. From this calculation we can clearly corroborate, again, that uncorrelated $2\pi/3$ propeller jumps are possible for $Me_3Sn(1)$ and $Me_3Sn(2)$ at room temperature. Whether or not this approximate 30% orientation dependence of the potential energy height at T = 178 K strictly requires correlated jumps—with low rates—at temperatures below 200 K, has to remain a matter of speculation: unfortunately, it was not possible to obtain meaningful kinetic NMR data at temperatures below 200 K. Still, the results of this calculation for the low temperature structure indicate that at low temperatures the two inequivalent reorienting Me_3Sn moieties in 1 should no longer be considered as truly independent of each other. The two-dimensional potential energy plot in Figure 5 also illustrates that maximum vdW oppression in 1 at T = 178 K occurs when the methyl groups of $Me_3Sn(1)$ are close to their crystallographic equilibrium positions: the maximum is reached when the C(3) methyl group of $Me_3Sn(1)$ lies almost in the plane defined by Sn(1)–O(5)–Sn(2), and when simultaneously $Me_3Sn(2)$ is rotated by approximately 60° from its equilibrium position. At this mutual orientation of $Me_3Sn(1)$ versus $Me_3Sn(2)$ the mutual methyl(1)–methyl(2) distance is minimized to approximately 2.85 Å. In contrast to this finding at T = 178 K, the equivalent maximum vdW oppression at T = 296 K only leads to an approximately 2.95 Å minimum distance.

In concluding, we would like to stress the important mutually supporting relationship between X-ray crystallography, solid-state NMR, and force field calculations for investigations of dynamic processes in crystalline molecular compounds in general. Even if compound 1, from a chemical point of view, is maybe not a particularly representative/general example from the enormously large number of known trimethyltin compounds, 1 is particularly suitable to exploit this multimethod approach. With respect to $2\pi/3$ reorientation in solid trimethyltin compounds in general, detailed mechanistic studies, where possible, are also required because similar reorientational processes have been reported for other types of polymeric solid trimethyltin compounds[12] and for a trimethylsilyl compound.[13]

Acknowledgment. Support of our work by the Deutsche Forschungsgemeinschaft and the Fonds der Chemischen Industrie is gratefully acknowledged. We would like to thank F. Seifert, Bayerisches Geoinstitut, for his continued support.

Supplementary Material Available: Tables of crystal data, atomic parameters, bond distances and angles, and thermal parameters (6 pages). Ordering information is given on any current masthead page.

OM9301391

(12) Apperley, D. C.; Davies, N. A.; Harris, R. K.; Eller, S.; Schwarz, P.; Fischer, R. D. *J. Chem. Soc., Chem. Commun.* **1992**, 740.

(13) Aliev, A. E.; Harris, K. D. M.; Apperley, D. C. *J. Chem. Soc., Chem. Commun.* **1993**, 251.